

This is a postprint version of the following published document:

Diez-Jimenez, E., Perez-Diaz, J., Ferdeghini, C., Canepa, F., Bernini, C., Cristache, C., Sanchez-Garcia-Casarrubios, J., Valiente-Blanco, I., Ruiz-Navas, E., & Martínez-Rojas, J. (2018). Magnetic and morphological characterization of Nd₂Fe₁₄B magnets with different quality grades at low temperature 5–300 K. *Journal of Magnetism and Magnetic Materials*, 451, 549–553.

DOI: <https://doi.org/10.1016/j.jmmm.2017.11.109>

© 2017 Elsevier B.V. All rights reserved.



This work is licensed under a [Creative Commons Attribution-NonCommercial-NoDerivatives 4.0 International License](https://creativecommons.org/licenses/by-nc-nd/4.0/).

Magnetic and morphological characterization of Nd₂Fe₁₄B magnets with different quality grades at low temperature 5-300 K

E. Diez-Jimenez^{a*}, J.L. Perez-Diaz^a, C. Ferdeghini^b, F. Canepa^{c,b}, C. Bernini^b, C. Cristache^c, J. Sanchez-Garcia-Casarrubios^c, I. Valiente-Blanco^c, E.M. Ruiz-Navas^d, J.A. Martínez-Rojas^a

^aMechanical Engineering Area, Signal Theory and Communications Department, Universidad de Alcalá, Spain 28341, Spain

^bCNR - SPIN, Corso Perrone 24, 16152 Genova, Italy

^cMAG SOAR SL, av. Europa 82, Valdemoro, Spain

^dMaterial Engineering department, Universidad Carlos III de Madrid, Leganés, Spain

^bUniversità degli studi di Genova, Genova, Italy

ARTICLE INFO

Article history:

Received

Received in revised form

Accepted

Available online

Keywords:

Cryogenic characterization

NdFeB magnets

Magnetic characterization

ABSTRACT

An increasing number of cryogenic devices may benefit from the use of Nd₂Fe₁₄B permanent magnets. However, it is necessary to precisely know their behavior because magnetization varies significantly due to Spin Reorientation Transition. In this work, magnetic and morphological characterization of Nd₂Fe₁₄B commercial polycrystalline magnets with different quality grades from 5 to 300 K is provided. A set of magnets ranging from N35 to N52 quality have been analyzed. Mean grain dimension as well as material composition elements are provided. Higher quality magnets show smaller mean grain dimensions. Regarding cryogenic temperatures, the well known spin transition effect appears in all the magnets as expected, however, the transition temperature occurs at different temperatures in a range from 112 to 120 K which is lower than those obtained for single crystal samples. Moreover, the relative variation of the remanence from 300 to 5 K is lower than 4% while the maximum expected variation is in average 11%. As extra information, the same analyzes are provided for additional quality grades N40M, N40S, N40SH and N40UH.

1. Introduction

Permanent magnets of Nd₂Fe₁₄B are probably the most popular magnets in technological devices operated at room temperature. This is mainly due to their high remanence and coercive field. Those properties are also demanded in cryogenic devices. A growing number of cryogenic devices are already including Nd₂Fe₁₄B polycrystalline permanent magnets [1–4]. However, Nd₂Fe₁₄B magnetic properties presents significant variations when decreasing the temperature. Like most of magnetic materials, magnetic saturation capacity increases when decreasing temperature. But specially, Nd₂Fe₁₄B structure suffers a spin-reorientation transition (SRT) at cryogenic which complicates the prediction of the expected behavior at low temperatures. Both effects must be known and taken into account during devices design process.

SRT is a temperature-induced magnetic phase transition that occurs at the Spin Tilt Temperature (T_{st}). It is characterized by a change of the Easy Magnetization Direction (EMD). For Nd₂Fe₁₄B at $T_{st} = 135$ K [5] the deviation of the EMD starts it changes from an “easy axis” anisotropy to an “easy cone” anisotropy, with a tilt angle increasing from 0° at 135 K to 31° at 0 K. Experimentally, the SRT of a Nd₂Fe₁₄B single crystal can be easily observed by a change in the slope in magnetization versus temperature measurements. Such a high tilt of the

magnetization must be carefully analyzed in the design of sensors, magnetic apparatus or magnetomechanical devices for cryogenic applications, whose working process is strongly affected by the direction of the magnetization vector. Most of those devices work with sintered Nd₂Fe₁₄B polycrystalline bulk magnets, thus a better understanding of the influence of the STR in macroscopic polycrystalline samples is needed.

Although SRT is well-known for Nd₂Fe₁₄B single crystals [6,7], there are very few papers describing experiments with polycrystalline samples [8–10] and none with commercial magnets. In this work, magnetic and morphological characterization of Nd₂Fe₁₄B commercial polycrystalline sample with different quality grades from 5 to 300 K is provided. A set of magnets ranging from N35 to N52 quality have been analyzed. As extra information, the same analyzes are provided for additional quality grades N40M, N40S, N40SH and N40UH.

2. Morphological characterization

A set of several Nd₂Fe₁₄B magnets with different quality grades was purchased. All the samples were cylinders with 3x3 mm size (diameter x length) with EMD axially polarized. All the samples were provided with Ni coating. Commercial polycrystalline magnets analyzed are provided with a classification according to Chinese standard.

A microscopic analysis of the samples was done. The images of the different samples were obtained by an optical microscope; the two images for several qualities are referred to two different cut sections, figure 1 and 2.

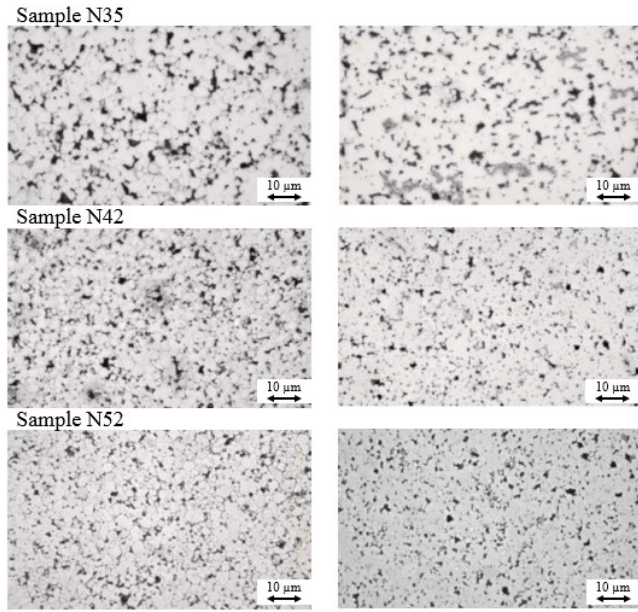


Figure 1. Microscopic images of N35, N42 and N52 samples. Images of two different cutting directions.

Immediately, it can be observed that lower quality sample N35 has much larger grain size than the other two. Moreover, the compactness of N35 sample is smaller since more and larger gaps can be appreciated at first sight. However, the difference between N42 and N52 is not significant. Table 1 is related to the mean grain dimension of the different Nd₂Fe₁₄B grades. The mean grain dimension has been obtained using the diagonal method.

Table 1. Mean grain dimension for N quality samples.

Sample	Mean grain dimension (μm)
N35	11.3±0.6
N42	7.3±0.2
N52	8.9±0.2

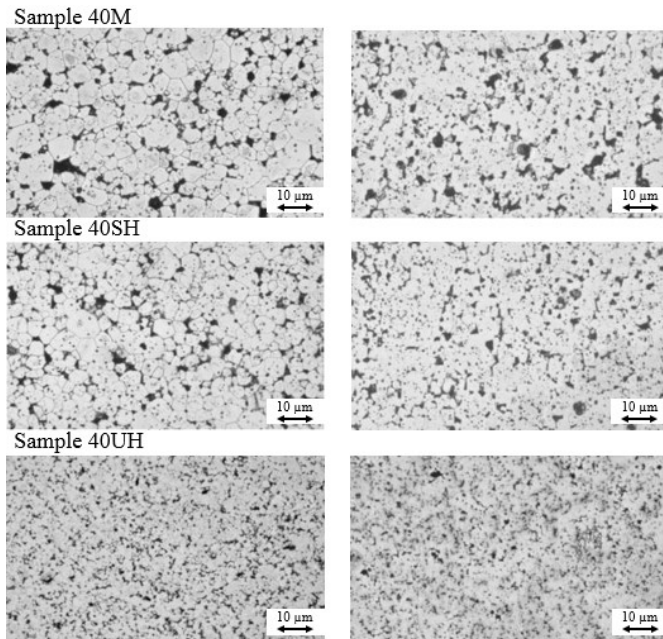


Figure 2. Images of N40M, N40SH and N40UH samples. Images of two different cutting directions.

Table 2 presents mean grain dimension of the different Nd₂Fe₁₄B grades N40M, SH and UH. The main difference in performance of these grades are their maximum working temperature which is 100°C for M class, 150°C for SH class and 180°C for UH class. Mean grain dimension does not affect significantly to the variation of maximum working temperature.

Table 2. Mean grain dimension for M, SH and UH quality samples.

Sample	Mean grain dimension (μm)
N40M	15.9±1.7
N40SH	15.5±3.3
N40UH	5.6±0.1

Additionally, semiquantitative analyses of the samples composition is provided in table 3. Boron is not included because can not be detected by the measurement instrument.

Table 3. Sample composition measurements (Atomic %).

Sample	Composition					
	Nd	Fe	Al	Pr	Dy	Co
N35	11.59	81.56	3.24	3.62	0	0
N52	10.69	85.99	0	3.33	0	0
N40M	14.58	83.07	1.63	0	0.73	0
N40SH	10.32	83.43	1.32	2.87	2.05	0
N40UH	9.18	81.49	0.85	2.88	2.69	2.91

From compositions analyses it is evident that the increase of the commercial grade from N35 to N52 in Nd₂Fe₁₄B permanent magnets corresponds to a decreasing of the Al content. This element is added to decrease the costs related to the production of the material, decreasing the melting temperature, while all the other processes remaining unchanged. The obvious consequence is an evident decrease of the magnetic properties related to the hysteresis cycle and thus, a decrease of the SRT temperature, as demonstrated next.

The increase of the working temperature, passing from 40M (Tw=100°C) to 40SH (Tw=150°C) and, finally, to 40UH (Tw=180°C) is related, from one side, to an increase in the Dy content. This increase leads to an increase of the melting temperature. Moreover, for 40UH sample, the addition of a small amount of Co instead of Fe, again further increases the melting temperature.

3. Magnetic characterization

3.1 Test set-up and data analysis procedure

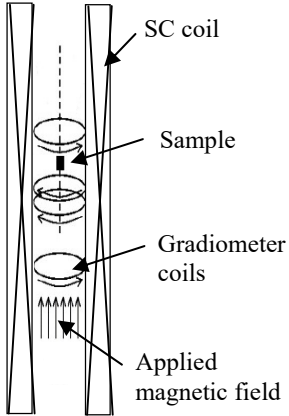
Amagnetometric study of Nd₂Fe₁₄B polycrystalline bulk magnets have been performed. The samples used were a cylindrical magnets of 3 mm in diameter and 3mm in height axially polarized.

All the magnetic measurements were performed

using a Superconducting Quantum Interference Device (SQUID) magnetometer, as part of a Magnetic Properties Measuring System (MPMS) by Quantum Design. The scheme and images of the system is depicted on figure 3. The SQUID-MPMS combines several superconducting components, including a SQUID, superconducting magnet, detection coils, flux transformer, and superconducting shields. In order to make a measurement, the sample is located to a sample rod holder. The sample is then scanned through the center of a superconducting gradiometer. This gradiometer forms a closed flux transformer that is coupled to a SQUID and the signal from the SQUID is typically recorded as a function of sample position. The shape

and magnitude of the response curve can then be analyzed using a computer to obtain the corresponding magnetic moment, m [11].

Figure 3. SQUID-MPMS scheme



In the case of the Nd₂Fe₁₄ samples, the magnetic remanence (B_R) value has been obtained for different temperatures. In order to calculate B_R from m the next procedure and expressions have been used (international system) :

$$B = \mu_o \cdot (H + M) \quad (1)$$

where M is the volumetric magnetization, H is magnetic field strength, B is the magnetic flux density and $\mu_o = 4\pi \times 10^{-7}$ H/m.

For the case of the magnetic remanence measurements, no external field will be applied to the magnets, $H = 0$ A/m. The absence of external magnetic field precludes the need of corrective demagnetizing factors. Thus, Volumetric magnetization M is straight forward given by the expression:

$$M = m_{sample} \cdot V_{sample} \quad (2)$$

Where m_{sample} is given by the SQUID-MPMS at different temperatures and V_{sample} is measured previously for each sample. Volumetric contraction has been considered negligible. Hence, magnetic remanence $B_R(T)$ can be written combining equation (1) and (2) in Teslas as:

$$B_R(T) = \mu_o \cdot (m_{sample}(T) \cdot V_{sample}) \quad (3)$$

The magnetic remanence, or DC Magnetization, absolute sensitivity of the system is 10^{-6} emu. The error on the measurements hereby reported is lower than 10^{-4} T thus not presented in the plots. The temperature range explored was 5-300 K for all the samples.

3.2 Characterization of N35-N52 magnets

The magnetic remanence temperature dependency has been obtained and plotted in figure 4. It has been obtained for the samples with qualities N35, N38, N40, N45, N48, N50 and N52.

During cooling down, two different behaviors can be described. Initially, remanence raises when decreasing the temperature because the self-alignment of magnetic domains favored by the reduction of thermal energy. However, at a certain temperature the slope of the tendency changes abruptly downwards and the remanence begins to fall. From this temperature the magnetization in the EMD decreases when

cooling down. This is known as SRT temperature. The decrease is due to a non-zero tilt angle of the cone of anisotropy that deviates the magnetization of every single crystal, reducing the total volumetric magnetization in the EMD. In any case, these effects acts on all the samples in a similar way, not finding any intersection between plots.

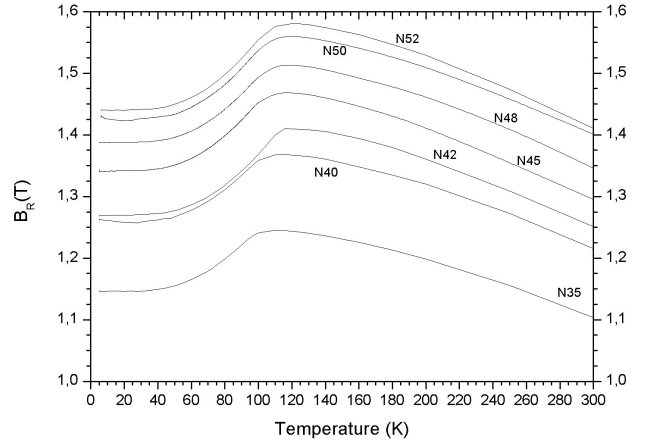


Figure 4. B_R versus Temperature for different quality grades N35-N52.

It is important to notice that the decrease so large that final values of the remanence at 5K are very close to those at 300K even though thermal energy highly reduced. In figure 5 the % of variation with respect to the initial remanence value at 300 is plotted. One symbols represent the variation at 5 K and the others represent the variation at the maximum remanence value (SRT temperature). The expressions for the calculation are:

$$\frac{B_R(T_{SRT}) - B_R(300)}{B_R(300)} \cdot 100 \quad \text{and} \quad \frac{B_R(5) - B_R(300)}{B_R(300)} \cdot 100$$

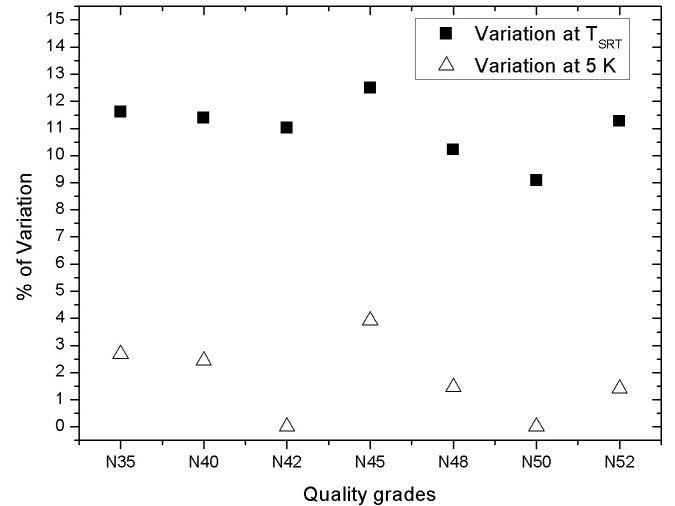


Figure 5. % of variation with respect to the initial remanence value for 5 K remanence and maximum remanence (T_{SRT}).

The finale remanence value with respect to initial one is in the range from 0 to 4% for the extreme case. The maximum variation or improvement that cooling down can provide for Nd₂Fe₁₄B commercial magnets is not larger than 12.5%. An 11% of remanence improvement can be considered as averaged for commercial polycrystalline magnets.

Moreover, a more detail analysis of the exact temperature where SRT occurs has been done. SRT temperature for the different grades N35-N52 is presented in figure 6.

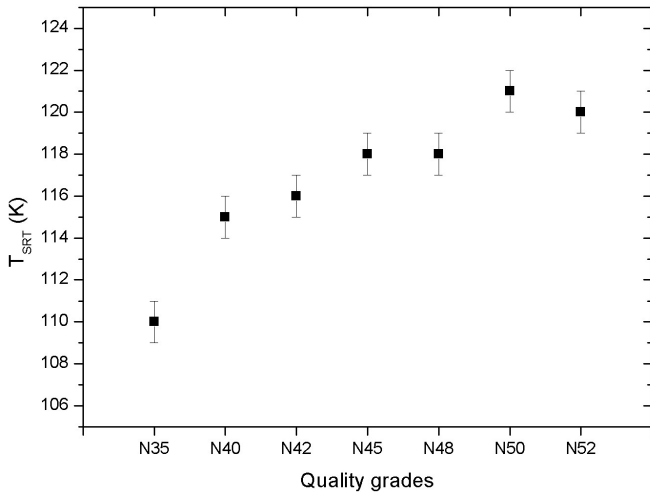


Figure 6. SRT temperature for the different grades N35-N52.

As already stated, Al content is added to decrease the costs related to the production of the material. An obvious consequence is an evident decrease of the magnetic properties related to the hysteresis cycle; moreover, a decrease of the SRT temperature, as shown in figure 6, is easily detected. For higher quality levels, Al content is progressively reduced down to 0 which favored the purity of the Nd₂Fe₁₄B sample increasing SRT temperature. It is noteworthy to see that the SRT temperature reported in literature for high purity (laboratory) Nd₂Fe₁₄B samples 135 K [12]. The decrease of SRT from 120 K (N52) down to 110K (N35) can be related to a decrease in the Nd – Nd interatomic distance, stabilizing thus the easy axis orientation.

Nevertheless, the values for the highest quality N52 is 120 K which is smaller than those obtained for single crystals or ribbons in previous references. This can be explained because in polycrystalline samples magnetic domains and grain boundaries retard the anisotropy cone apparition.

3.3 Characterization of N40-M-H-SH-N40UH magnets

The magnetic remanence temperature dependency has been obtained and plotted in figure 7. It has been obtained for the samples with qualities N40, N40M, N40H, N40SH and N40UH.

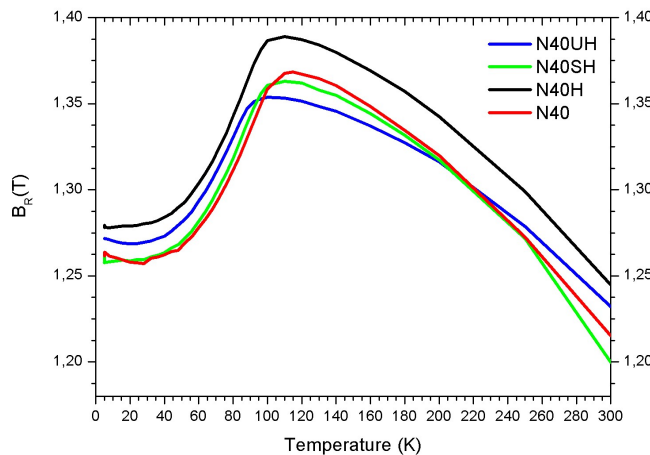


Figure 7. B_r versus Temperature for different quality grades N40-H-SH-N40UH, (N40M quality values are not included because lack of measurement points).

The same two behaviors before and after SRT can be observed. There is not a dependency in the room temperature with respect to the different grades.

However, it is significant that the remanence varies differently when cooling down depending on the quality. N40 curve intersects with those from N40H and N40UH in several points. For higher temperatures magnets, dysprosium is a key element as shown in table 2. Dysprosium have one of the highest magnetic strengths of the elements, especially at low temperatures [13]. Dysprosium has a simple ferromagnetic ordering at temperatures below 85 K. Above 85 K, it turns into an helical antiferromagnetic state in which all of the atomic moments in a particular basal plane layer are parallel. This unusual antiferromagnetism transforms into a disordered (paramagnetic) state at 179 K. Therefore, it can be expected different slopes between N40 (dysprosium free) and the rest of the high temperature qualities as shown in figure 7

In figure 8 the % of variation with respect to the initial remanence value at 300 it is plotted. Some symbols represent the variation at 5 K and the second symbols represent the variation at the maximum remanence value (SRT temperature).

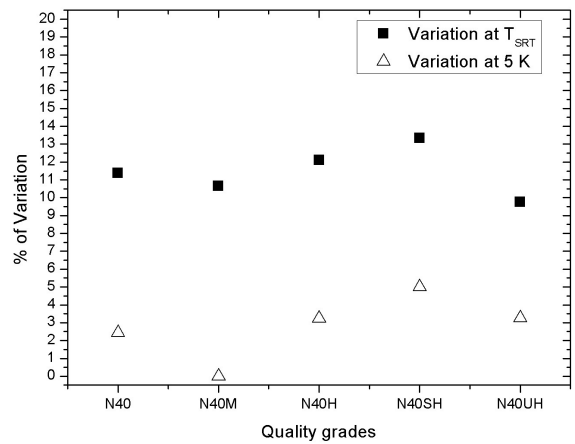


Figure 8. % of variation with respect to the initial remanence value for 5 K remanence and maximum remanence (T_{SRT}) for high temperature magnets.

The variations for high temperature magnets are quite similar to those for N grades. The mean maximum variation is also located at 11% while the difference between 300 and 5 is in the 0-5% range.

At last, a more detail analysis of the exact temperature where SRT occurs has been also done for high temperature magnets.

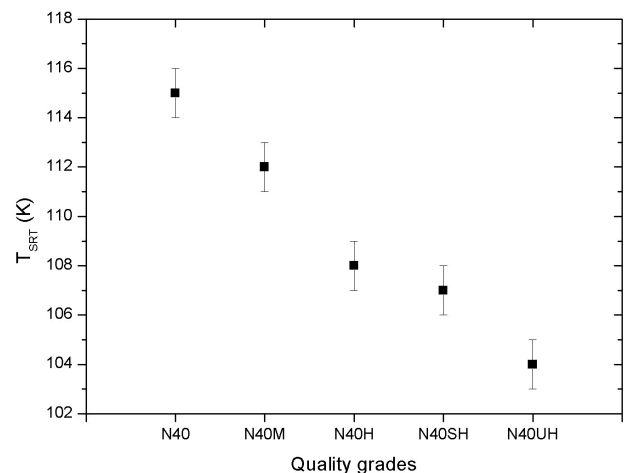


Figure 9. SRT temperature for the different grades different quality grades N40-H-SH-N40UH.

Figure 9 show a clear dependency on the SRT temperature that decreases when increasing working maximum temperature. This is assumed to be due to the increase of dysprosium and cobalt content in the higher temperature magnets. Again, the substitution of Nd^{3+} ($r = 0.995 \text{ \AA}$) by a smaller RE ion (Dy^{3+} with $r = 0.912 \text{ \AA}$) seems to decrease the rare earth – rare earth interatomic distance, favoring thus the stability of the *easy axis* preferred magnetization direction.

4. Conclusion

An increasing number of cryogenic devices may benefit from the use of Nd2Fe14B permanent magnets. However, it is necessary to precisely know their behavior because magnetization varies significantly due to Spin Reorientation Transition.

In this work, magnetic and morphological characterization of Nd2Fe14B commercial polycrystalline magnets with different quality grades from 5 to 300 K is provided. A set of magnets ranging from N35 to N52 quality have been analyzed. Mean grain dimension as well as material composition elements are provided. Higher quality magnets show smaller mean grain dimensions. Regarding cryogenic temperatures, the well know spin transition effect appears in all the magnets as expected, however, the transition temperature occurs at different temperatures in a range from 112 to 120 K which is lower than those obtained for single crystal samples. Moreover, the relative variation of the remanence from 300 to 5 K is lower than 4% while the maximum expected variation is in average 11%. As extra information, the same analyzes are provided for additional quality grades N40M, N40S, N40SH and N40UH.

The values presented in these figures can be very useful for accurate magnetic design of devices operating in cryogenic environments. The selection of the quality of the permanent magnets must take into consideration the variations of the magnetization with temperature.

Acknowledgments

The research leading to these results has received funding from the European Community's Seventh Framework Programme ([FP7/2007-2013]) under grant agreement n° 263014.

References

- [1] J.L. Perez-Diaz, E. Diez-Jimenez, Performance of Magnetic-Superconductor Non-Contact Harmonic Drive for Cryogenic Space Applications, *Machines*. 3 (2015) 138–156. doi:10.3390/machines3030138.
- [2] J.L. Perez-Diaz, I. Valiente-Blanco, E. Diez-Jimenez, J. Sanchez-Garcia-Casarrubios, Superconducting Non-Contact Device for Precision Positioning in Cryogenic Environments, *IEEE/ASME Trans. Mechatronics*. 19 (2014) 1–8. doi:10.1109/TMECH.2013.2250988.
- [3] E. Diez-Jimenez, J.-L. Perez-Diaz, J.C. Garcia-Prada, Local model for magnet–superconductor mechanical interaction: Experimental verification, *J. Appl. Phys.* 109 (2011) 63901–63901–5. doi:doi:10.1063/1.3553581.
- [4] I. Valiente-Blanco, E. Diez-Jimenez, Characterization and Improvement of Axial and Radial Stiffness of Contactless Thrust Superconducting Magnetic Bearings, *Tribol. Lett.* (2014). <http://link.springer.com/article/10.1007/s11249-013-0204-0> (accessed September 11, 2014).
- [5] M. Foldeaki, L. Koszegi, R.A. Dunlap, Structure sensitivity of magnetization processes at the spin-reorientation transition in Nd2Fe14B, *J. Appl. Phys.* 69 (1991) 5562–5564. doi:10.1063/1.347950.
- [6] F.E. Pinkerton, Spin reorientation in melt-spun neodymium-iron-boron ribbons, *J. Appl. Phys.* 64 (1988) 5565–5567.
- [7] X.C. Kou, M. Dahlgren, R. Grössinger, G. Wiesinger, Spin-reorientation transition in nano-, micro- and single-crystalline Nd2Fe14B, *J. Appl. Phys.* 81 (1997) 4428. doi:10.1063/1.364791.
- [8] E. Diez-Jimenez, J.L. Perez-Diaz, F. Canepa, C. Ferdeghini, Invariance of the magnetization axis under spin reorientation transitions in polycrystalline magnets of Nd2Fe14B, *J. Appl. Phys.* 112 (2012) 63918. doi:10.1063/1.4754445.
- [9] D. Givord, P. Tenaud, T. Viadieu, Analysis of hysteresis loops in Nd-Fe-B sintered magnets, *J. Appl. Phys.* 60 (1986) 3263–3265.
- [10] A.S. Lileev, A.A. Parilov, M. Reissner, W. Steiner, Influence of the spin reorientation transition on the hysteresis characteristics of Nd-Fe-B film and bulk magnets, *J. Magn. Magn. Mater.* 270 (2004) 152–156. doi:10.1016/j.jmmm.2003.08.012.
- [11] R.C. Black, F.C. Wellstood, Measurements of Magnetism and Magnetic Properties of Matter, in: *SQUID Handb. Appl. SQUIDS SQUID Syst.*, 2006: pp. 391–440. doi:10.1002/9783527609956.ch12.
- [12] J.M.D. Coey, *Rare Earth Iron Permanent Magnets*, Oxford, 1996.
- [13] R.E. Krebs, *The History and Use of Our Earth's Chemical Elements: A Reference Guide*, 2006.